ARTICLE

Fabrication of Pt/Au Concentric Spheres from Triblock Copolymer

Haeng-Deog Koh,[†] Soojin Park,[‡] and Thomas P. Russell[†,*]

[†]Department of Polymer Science and Engineering, University of Massachusetts, Amherst, Massachusetts 01003 and [‡]School of Energy Engineering, Ulsan Institute of Science and Technology, Ulsan 689-798, Korea

ABSTRACT Dispersion of an aqueous H_2PtCl_6 solution into a trifluorotoluene (TFT) solution of a polystyrene-*block*-poly(2-vinylpyridine)-*block*-poly(ethylene oxide) (PS-*b*-P2VP-*b*-PEO) triblock copolymer produced an emulsion-induced hollow micelle (EIHM), comprising a water nanodroplet stabilized by PEO, H_2PtCl_6/P2VP, and PS, sequentially. The following addition of an aqueous $LiAuCl_4$ solution into the dispersion led to a coordination of $LiAuCl_4$ and PEO. The resulting spherical EIHM structure was transformed to a hollow cylindrical micelle by the fusion of spherical EIHM with the addition of methanol. This structural transition was reversible by the alternative addition of methanol and TFT. Oxygen plasma was used to generate Pt/Au concentric spheres and hollow cylindrical Pt/Au nano-objects.

KEYWORDS: block copolymer · hollow micelle · bimetallic metal · concentric sphere

Block copolymers (BCPs) can aggregate into spherical,[1] cylindrical,[2] or hollow micelles (or vesicles),[3] or lamellar phases[4] depending on the concentration of solvents, the solubility of the blocks in the solvents, the immiscibility of the solvents, and the asymmetry of the BCP. For example, solvation of BCP in a solvent that is selective to one of blocks can lead to formation of spherical micelles with an insoluble block core and a soluble block shell. When the core consists of a functional block, like poly(2-vinylpyridine) (P2VP)[5] or poly(ethylene oxide) (PEO),[6] that can be coordinated with metallic or semiconductor precursors, these micelles can be used as templates or scaffolds for preparing metallic, semiconductor nanoparticles (NPs) and quantum dots. The shape of the micelle, of course, controls the shape of the resultant nano-objects, be it a sphere, sheet or rod, solid or hollow. The shape of the nanoscopic objects dictate the optical, magnetic, electronic, and catalytic properties.[7−9] Furthermore, the spatial distribution of the nanoscopic objects in a film will also influence the physical and chemical properties of the nanostructured composite materials.[10,11]

BCPs can be used as a surfactant to stabilize mixed solvent systems; of particular interest to our studies are systems composed of water dispersion in an organic solvent.[12−14] For example, the dispersion of water in toluene can be stabilized with a polystyrene-*block*-poly(2-vinylpyridine) (PS-*b*-P2VP) and, in fact, a stable emulsion-induced hollow micelle (EIHM) can form with the BCP at the interface between the two immiscible fluids.[15] Casting films of such dispersion results in the formation of a continuous PS matrix with pores bounded by P2VP. Such films can be used as microencapsulates for drugs delivery or as nanoreactors for synthesizing metallic or semiconductor NPs and quantum dots.[16,17]

Recently, polystyrene-*block*-poly(2-vinylpyridine)-*block*-poly(ethylene oxide) (PS-*b*-P2VP-*b*-PEO) ABC triblock copolymer has been used to synthesize bimetallic NPs because of the ability to coordinate the PVP and PEO with different metallic precursors.[18−22] Buriak and co-workers demonstrated that a $HAuCl_4$ precursor was selectively coordinated with P2VP, while $AgNO_3$ was exclusively complexed with the PEO block.[23] Consequently, the Au/Ag bimetallic nanodots and wire arrays could be fabricated. Sohn and co-workers also reported the generation of Fe/Au bimetallic NPs by the coordination of $FeCl_3$ with P2VP and $LiAuCl_4$ with PEO.[24] However, the structure and size distribution of NPs was irregular and broad.

Herein, we report the dispersion of H_2PtCl_6 aqueous solutions into organic triblock copolymer solutions, followed by the dispersion of $LiAuCl_4$ aqueous

*Address correspondence to russell@mail.pse.umass.edu.

Received for review November 11, 2009 and accepted January 20, 2010.

Published online January 29, 2010. 10.1021/nn9016026

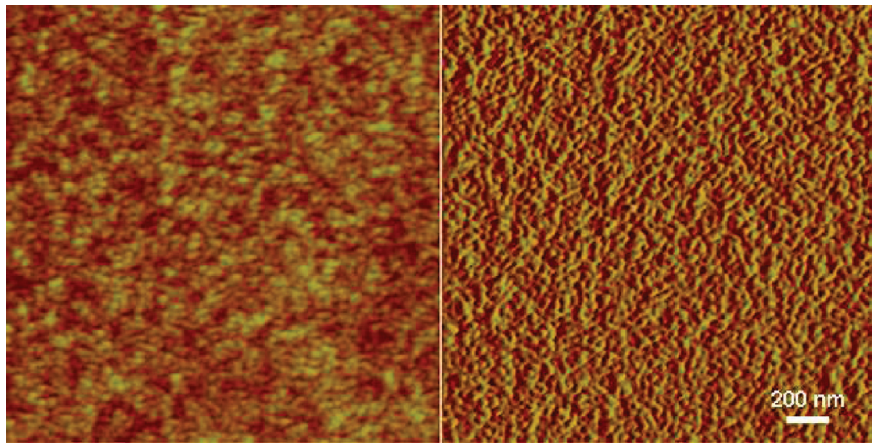

Figure 1. SFM (left, height; right, phase) image of a PS-*b*-P2VP-*b*-PEO spin-coated from TFT polymer solution.

solutions into the Pt-loaded polymer solutions that leads to the formation of the unique EIHM nanostructures, a water nanodroplet stabilized by $LiAuCl_4$/PEO, H_2PtCl_6/P2VP, and PS. The structural transition of the spherical EIHMs into the cylindrical shaped hollow micelles by an intermicellar fusion is demonstrated. The synthesis of a Pt/Au bimetallic concentric sphere and a hollow cylindrical nano-object with regular size and shape is also shown.

RESULTS AND DISCUSSION

Formation of Emulsion-Induced Hollow Micelles (EIHMs). Figure 1 shows a scanning force microscopic (SFM) image of a PS-*b*-P2VP-*b*-PEO spin-coated from TFT polymer solution. Even though a selective solvent, TFT, for PS block, was used, the nano-object formed was random and irregular with wormlike nanostructure. The average diameter of this nano-object was ~50 nm.

The addition of metallic precursors such as $HAuCl_4$, $LiAuCl_4$, and H_2PtCl_6 into TFT-based polymer solution led to formation of more distinct nanoscopic objects having a spherical shape. The adjustment of aqueous metallic solutions, instead of salts themselves, produced stable EIHM structure with uniform size and shape. Considering the coordination preference of the metallic precursors, H_2PtCl_6 and $LiAuCl_4$, which resulted in the complexation of H_2PtCl_6/P2VP and $LiAuCl_4$/PEO, the synthetic pathway of the formation of Pt/Au concentric sphere nano-objects can be illustrated as shown in Scheme 1. Addition of a predetermined amount of aqueous H_2PtCl_6 solution to the TFT solution of PS-*b*-P2VP-b-PEO resulted in stable, well-defined EIHMs with the H_2PtCl_6/P2VP complex. Here, the H_2PtCl_6 metallic precursor is predominately coordinated by the pyridine group of the P2VP, but not the PEO. The existence of a dispersed water minor phase in the TFT major phase plays a key role in the microphase separation of PEO and P2VP. Here, the PEO is soluble in the water, while the PS is soluble in TFT. The complexed P2VP, on the other hand, is insoluble in both solvents and, as such, is positioned at the middle layer between PEO and PS. The subsequent addition of the $LiAuCl_4$ metallic precursor allows easy access to the PEO block enabling the formation of the ($LiAuCl_4$/PEO) complex. In this manner, a layered structure is imparted to the two different complexes allowing the formation of the Pt/Au bimetallic concentric sphere nano-objects.

Pt Concentric Spheres. Figure 2 shows the SFM and TEM images of a PS-*b*-H_2PtCl_6/P2VP-*b*-PEO EIHM complex. The distinct spherical shape of the EIHMs

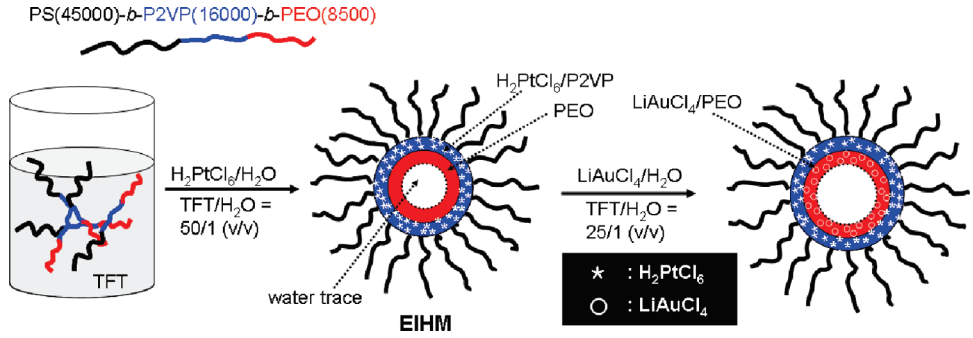

Scheme 1. Formation of an emulsion-induced hollow micelle (EIHM). Aqueous H_2PtCl_6 and $LiAuCl_4$ solutions were dispersed into the TFT solution of PS-*b*-P2VP-b-PEO, one after the other. First, H_2PtCl_6 (✻) coordinates with the pyridine group of the P2VP, not the PEO, and then $LiAuCl_4$ (○) is exclusively coordinated with the PEO block

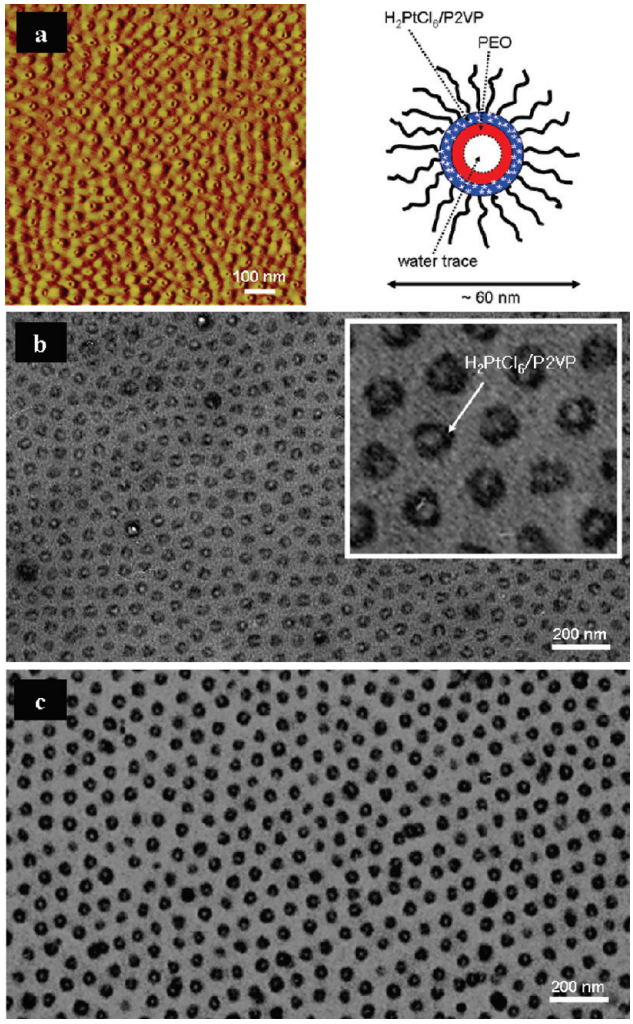

Figure 2. (a) SFM, (b) nonstaining, and (c) I_2-staining TEM images of a PS-*b*-H_2PtCl_6/P2VP-*b*-PEO EIHM structure. I_2 selectively stains the P2VP domains.

was seen with a diameter of ~60 nm. The depression in the center of the objects results from the evaporation of water in the center of the spheres during drying. Although the TEM specimen was not stained (Figure 2b), the dark nanorings are clearly observed due to the huge contrast of electron density between metal/polymer and air. Again, this is consistent with the P2VP being complexed with the Pt precursor forming a layer around the water phase and, upon drying, the spheres collapse leaving a ring of the higher electron density Pt. Consequently, the regularity in size and shape of EIHMs with a diameter of ~60 nm is evidenced by these results. After staining the EIHM nanostructure by iodine (I_2), the H_2PtCl_6-coordinated P2VP domain appeared much darker (Figure 2c). It was well-known that I_2 can stain selectively the P2VP domain. It clearly indicated that the H_2PtCl_6 precursor was exclusively coordinated with the P2VP block.

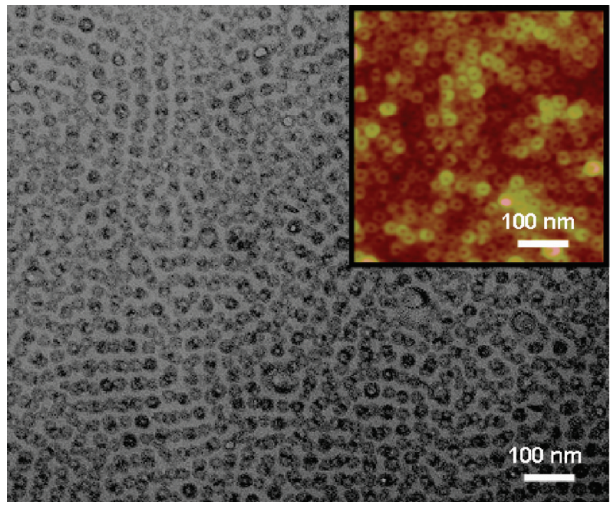

Figure 3. TEM (inset: SFM) image of pure Pt concentric sphere nano-objects after removing the polymer by O_2 plasma.

Figure 3 shows the TEM (inset: SFM) image of the dried films after O_2 plasma treatment which removes all the organics. In keeping with the results discussed above, the plasma treatment led to the formation of Pt concentric spheres with an average size of ~30 and thickness of ~10 nm. The reduction in the size of the nanorings arises from a loss of the organics and the formation of Pt metal.

Pt/Au Bimetallic Concentric Spheres. A predetermined amount of an aqueous $LiAuCl_4$ solution was added to the TFT-based solution of PS-*b*-H_2PtCl_6/P2VP-*b*-PEO. Since the H_2PtCl_6 metallic precursor was already coordinated with the P2VP block, the $LiAuCl_4$ was exclusively coordinated with the PEO block. This formed EIHMs of PS-*b*-H_2PtCl_6/P2VP-*b*-$LiAuCl_4$/PEO. SFM and TEM images of the dried EIHMS are shown in Figure 4. The SFM image (Figure 4a) closely resembles the structures seen when only the P2VP was complexed where the collapse of a metal/polymer concentric nano-object forms a ringlike structure.[25] However, the TEM image (Figure 4b), on the other hand, shows an electron dense Pt nanoring, as discussed above, but with a much darker, more electron dense, region in the center, due to the Au complexed with the PEO core inside Pt/P2VP. It should be noted that the shape of the Au in the center is irregular, sometimes with a line forming in the center. This is fully consistent with the collapse of a spherical object within another spherical object where folds in the interior sphere can easily form.

Studies were also performed with the TFT:H_2O volume ratio (v/v) changed from 50:1 (PS-*b*-H_2PtCl_6/P2VP-*b*-PEO) to 25:1 (PS-*b*-H_2PtCl_6/P2VP-*b*-$LiAuCl_4$/PEO). With increasing the H_2O content, the sizes of EIHMs also increased. The average size of PS-*b*-H_2PtCl_6/P2VP-*b*-$LiAuCl_4$/PEO EIHMs was ~90 nm from 25:1 (TFT:H_2O, v/v), while that of PS-*b*-H_2PtCl_6/P2VP-*b*-PEO EIHMs from 50:1 (TFT:H_2O, v/v) was ~60 nm (Figure 2).

Figure 5 shows the TEM (inset: SFM) image of the Pt/Au bimetallic concentric sphere nano-object. The

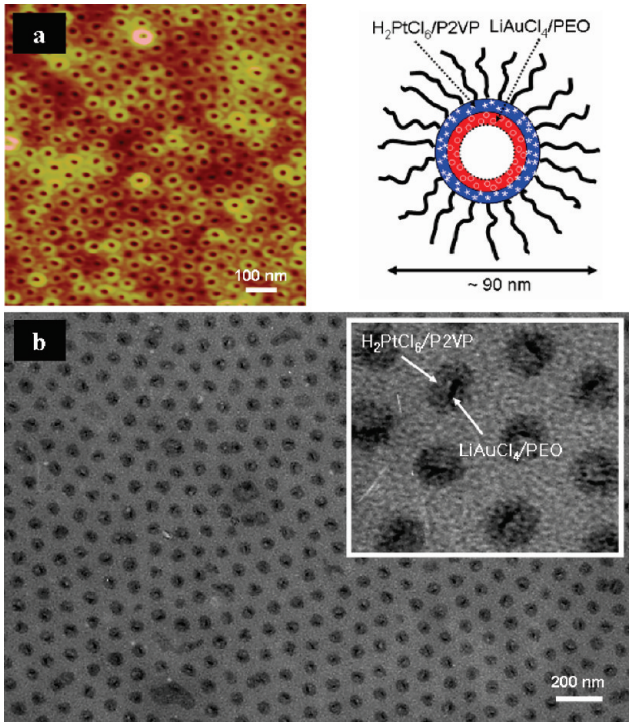

Figure 4. (a) SFM and (b) TEM images (without staining) of a PS-*b*-H_2PtCl_6/P2VP-*b*-$LiAuCl_4$/PEO.

PS-*b*-H_2PtCl_6/P2VP-*b*-$LiAuCl_4$/PEO EIHM complex deposited on the substrate was treated with O_2 plasma to remove the polymer and to reduce both metal cations to pure metal. The average size of Pt/Au bimetallic nanorings was ~60 nm with a thickness of ~15 nm, approximately 5 nm thicker than that seen with the Pt monometallic concentric sphere.

The surface plasmon resonances (SPRs) of Au, Pt, and Pt/Au concentric sphere nano-objects on quartz cells were characterized by UV−Vis absorption. Au concentric spheres were prepared by dispersing the aqueous $HAuCl_4$ solution into H_2PtCl_6/P2VP complexed dispersion, casting onto quartz cells, and followed by an O_2 plasma treatment. It was well-known that a maximum absorption wavelength consistent with the SPR of Au NPs was seen from 500−550 nm, where the intrinsic SPR absorption band for Pt NPs was absent. It was also recently reported that no SPR absorption characteristic of Pt/Au bimetallic NPs was observed regardless of Au:Pt ratio while a Au SPR maximum wavelength of an absorption band was seen at 500−550 nm for physical mixtures of Pt and Au NPs, where the absorption intensity is proportional to the concentration of Au NPs.[26] As shown in Figure 6, the Au nanoring-like objects showed the SPR absorption peak at 520 nm, while no absorption characteristic of Pt was evident. In the case of Pt/Au nanoring-like objects, the Au-based SPR absorption bands were not observed, regardless of Au:Pt ratio. Au/Pt-1 contained more Au (from 0.6 molar ratio $LiAuCl_4$ per PEO unit) in comparison to Au/Pt-2 (from 0.3 molar ratio LiAuCl4 per PEO unit) relative to the Pt content. This strongly indicates that the concentric sphere nano-objects are Au/Pt hybrids and not a simple physical mixture of the two.

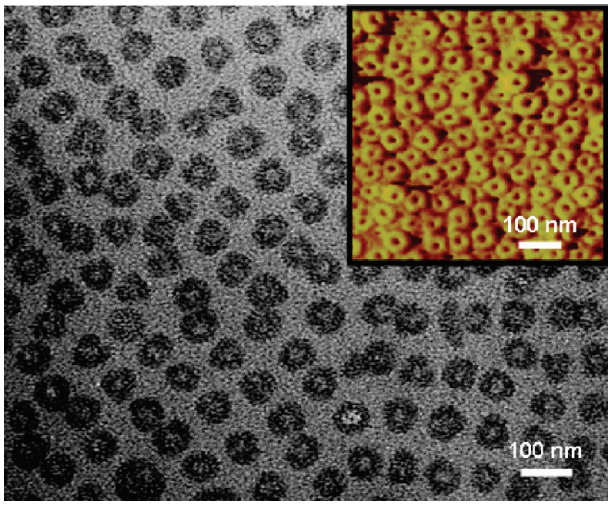

Figure 5. TEM (inset: SFM) image of Pt/Au bimetallic concentric sphere nano-objects after removing the polymer by adjusting O_2 plasma.

Structural Transition of a Spherical to a Cylindrical EIHM Structure. Synthesis of Cylindrically Hollow Pt/Au. Recently, Gohy and co-workers demonstrated that core cross-linked spherical BCP micelles were structurally transformed into the rodlike micellar structures by controlling solvent composition.[27] Core-cross-linking was used for structural stability in the presence of external stimuli, like pH, temperature, and solvent composition.

The complexation of H_2PtCl_6/P2VP and $LiAuCl_4$/PEO in EIHM nanostructure also stabilizes the P2VP (corona) and PEO (core) domains. The complexation served a similar function to the core-cross-linking. The addition of methanol into the TFT-based solution of a PS-*b*-H_2PtCl_6/P2VP-*b*-$LiAuCl_4$/PEO EIHM complex can induce an expansion of complexed H_2PtCl_6/P2VP and $LiAuCl_4$/PEO, and consequently the spherical EIHMs can be transformed into hollow cylindrical shapes by an intermicellar fusion, as illustrated in Scheme 2. Figure 7 panels a and b show SFM and TEM images (no staining) of hollow cylindrical EIHMs, though hollow spherical micelles are also evident. The widths and lengths of the hollow cylindrical EIHMs were estimated to be ~90 nm (consistent with the diameter of spherical EIHMs) and ~300 nm, respectively, by AFM and TEM. The structural transition between spherical and cylindrical EIHMs was reversible by the alternate addition of methanol (1 mL) and TFT (5 mL) into the TFT solutions of hollow cylindrical EIHMs

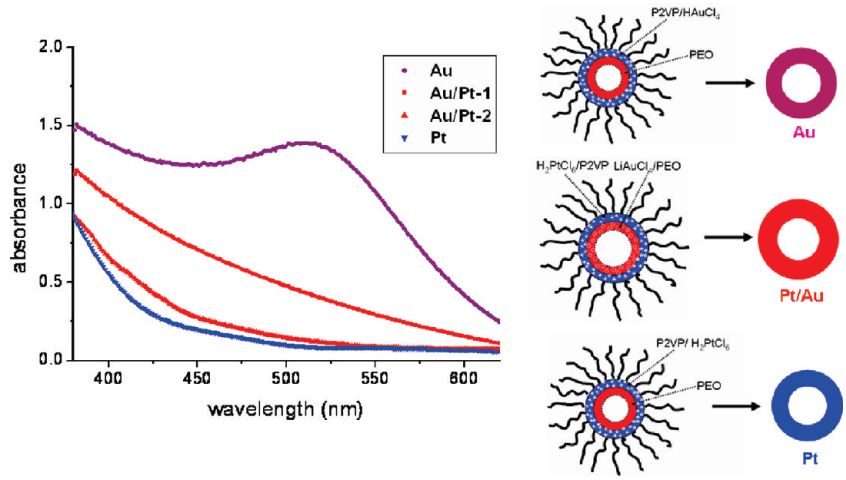

Figure 6. UV−Vis absorption spectrum of Au, Pt/Au, and Pt concentric sphere nano-objects prepared on quartz substrate.

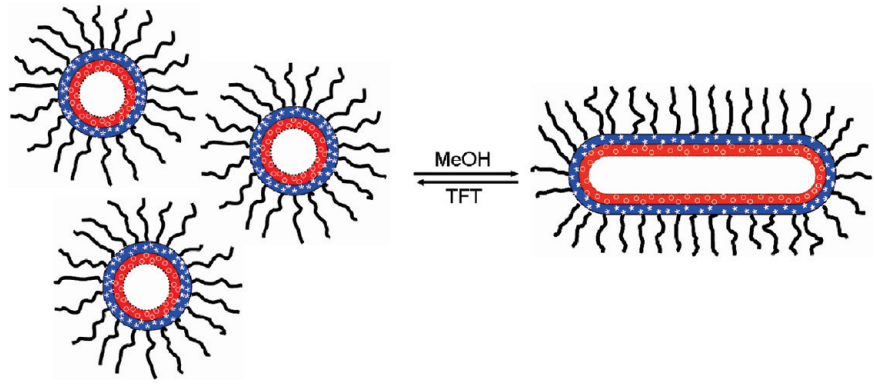

Scheme 2. Schematic illustration of a reversible transformation between a spherical and a cylindrical EIHM by the alternative addition of methanol and TFT to the EHIM solution.

(0.5 wt % concentration, 5 mL). The sizes and shapes of spherical and cylindrical EIHMs could be confirmed by a triple repetition of methanol/TFT addition. With more repetition, this procedure produced undistinguished nano-objects instead of spherical and cylindrical EIHMs due to the low polymer concentrations and insufficient water minor phase for constructing EIHMs in the TFT/methanol major phase.

When a PS-*b*-H_2PtCl_6/P2VP-*b*-$LiAuCl_4$/PEO cylindrical EIHM complex was spin-coated onto a substrate and treated with an O_2 plasma, hollow cylindrical Pt/Au nano-objects were observed with a small amount of hollow spherical nano-objects (Figure 7c). The exposure to an O_2 plasma results in the uncontrolled fusion of hierarchically hollow cylindrical Pt/Au nano-objects (Figure 7d) with an average diameter of ~60 nm and thickness of ~15 nm.

CONCLUSIONS

We have demonstrated that the sequential addition of an aqueous H_2PtCl_6 and $LiAuCl_4$ solutions to a TFT-based PS-*b*-P2VP-*b*-PEO solution formed a complexed EIHM structure encasing a water nanodroplet. Comparison of an aqueous H_2PtCl_6 solution (TFT/H_2O = 50:1, v/v) with an aqueous $LiAuCl_4$ (TFT/H_2O = 25:1, v/v) solution, showed that the size of EIHM structures can be varied from ~60 nm to ~90 nm with inner diameters of ~20 nm to ~40 nm, respectively. Well-defined Pt and Pt/Au nanoring-like objects were formed by an O_2 plasma treatment. Spherical H_2PtCl_6/$LiAuCl_4$-coordinated EIHMs could be transformed into cylindrical structures, by fusion when methanol was added into the solution, that were used as templates to generate hollow cylindrical Pt/Au nanostructures. The methodology demonstrated here extends the use of triblock copolymers to synthesize and control the shape and complexity of NPs.

EXPERIMENTAL SECTION

Materials. Polystyrene-*block*-poly(2-vinylpyridine)-*block*-poly (ethylene oxide) (PS-*b*-P2VP-*b*-PEO) ABC triblock copolymers with molecular weight (M_n) of PS (45 kg/mol), P2VP (16 kg/mol), and PEO (1.6 kg/mol) and its polydispersity with 1.06 was purchased from Polymer Source. α,α,α-trifluorotoluene (TFT) (99.9%, from Aldrich), which is a selective solvent for the majority of PS block, was used to solvate the triblock copolymer. Hydrogen hexachloroplatinate (IV)

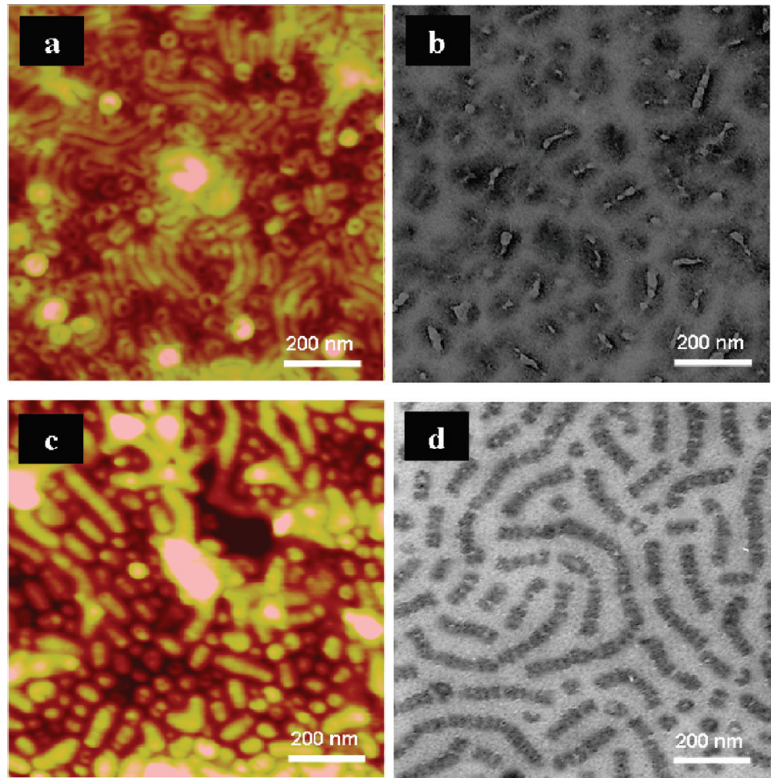

Figure 7. SFM (left) and TEM (right) images of (a,b) a cylindrical EIHM structure obtained by adding methanol into the TFT solution of spherical PS-*b*-H_2PtCl_6/P2VP-*b*-$LiAuCl_4$/PEO EIHMs and (c,d) hollow cylindrical Pt/Au nano-objects after removing the polymer by O_2 plasma treatment.

(H_2PtCl_6) hydrate (from Fluka) and lithium tetrachloroaurate (III) ($LiAuCl_4$) (from Aldrich) were used as metallic precursors.

Preparation of EIHMs and Synthesis of Pt/Au Concentric Spheres. PS-*b*-P2VP-*b*-PEO was dissolved in TFT to make 0.5 wt % polymer solution at room temperature. The polymer solution was heated to 60 °C for 1 h and cooled slowly to room temperature. This process was repeated several times. Then, an aqueous H_2PtCl_6 solution was added into the polymer solution (molar ratio of H_2PtCl_6 and pyridine units was 1:1, volume ratio of water/TFT was 1/50) and the mixed solution was stirred for 24 h at room temperature. Here, note that addition of an aqueous precursor solution enhances the coordination with the P2VP compared with the case of a solid salt, itself. Then an aqueous $LiAuCl_4$ solution was dispersed into the EIHM solution with H_2PtCl_6/P2VP (molar ratio of $LiAuCl_4$ and EO units was 0.3:1, volume ratio of water/TFT was 1/25). The resulting solution was also stirred for 1 h and filtrated with membrane filter having 0.45 μm pores. The EIHM solution with H_2PtCl_6/P2VP and $LiAuCl_4$/PEO was spin-coated on Si-water or quartz substrate at 3000 rpm for 60 s. The resulting substrate was treated with O_2 plasma to remove the polymer and to obtain Pt/Au pure metals.

Characterization. The solutions were drop-coated on silicon nitride (Si_3N_4) windows for investigation by transmission electron microscope (JEOL-1200EX). The TEM analysis was operated at an accelerating voltage of 100 kV. The surface topography of various nanostructures was imaged by SFM (Digital Instruments, Nanoscope III) in the tapping mode.

Acknowledgment. This work was supported by the Department of Energy Office of Basic Energy Sciences. S. Park was supported by WCU (R31-2008-000-20012-0) Program.

REFERENCES AND NOTES

1. Förster, S.; Antonietti, M. Amphiphilic Block Copolymers in Structure-Controlled Nanomaterial Hybrids. *Adv. Mater.* **1998**, *10*, 195–217.
2. Zhang, M.; Drechsler, M.; Müller, A. H. E. Template-Controlled Synthesis of Wire-like Cadmium Sulfide Nanoparticle Assemblies within Core−Shell Cylindrical Polymer Brushes. *Chem. Mater.* **2004**, *16*, 537–543.
3. Jenecke, S. A.; Chen, L. Self-Assembly of Ordered Microporous Materials from Rod−Coil Block Copolymers. *Science* **1999**, *283*, 372–375.
4. Wang, J.-Y.; Chen, W.; Roy, C.; Sievert, J. D.; Russell, T. P. Influence of Ionic Complexes on Phase Behavior of Polystyrene-*b*-poly(methyl methacrylate) Copolymers. *Macromolecules* **2008**, *41*, 963–969.
5. Park, S.; Kim, B.; Cirpan, A.; Russell, T. P. Preparation of Metallic Line Patterns from Functional Block Copolymers. *Small* **2009**, *5*, 1343–1348.
6. Kim, S. H.; Misner, M. J.; Yang, L.; Gang, O.; Ocko, B. M.; Russell, T. P. Salt Complexation in Block Copolymer Thin Films. *Macromolecules* **2006**, *39*, 8473–8479.
7. Li, C.-P.; Wei, K.-H.; Huang, T. Y. Enhanced Collective Electron Transport by CdSe Quantum Dots Confined in the Poly(4-vinylpyridine) Nanodomains of a Poly(styrene-*b*-4-vinylpyridine) Diblock Copolymer Thin Film. *Angew. Chem., Int. Ed.* **2006**, *45*, 1449–1453.
8. Wang, D.; Cao, Y.; Zhang, X.; Liu, Z.; Qian, X.; Ai, X.; Liu, F.; Wang, D.; Bai, Y.; Li, T.; Tang, X. Size Control of CdS Nanocrystals in Block Copolymer Micelle. *Chem. Mater.* **1999**, *11*, 392–398.
9. Chen, D.; Park, S.; Chen, J.-T.; Redston, E.; Russell, T. P. A Simple Route for the Preparation of Mesoporous Nanostructures Using Block Copolymers. *ACS Nano* **2009**, *3*, 2827–2833.
10. Sohn, B.-H.; Choi, J.-M.; Yoo, S.-I.; Yun, S.-H.; Zin, W.-C.; Jin, J.-C.; Kanehara, M.; Hirata, T.; Teranish, T. Directed Self-Assembly of Two Kinds of Nanoparticles Utilizing Monolayer Films of Diblock Copolymer Micelles. *J. Am. Chem. Soc.* **2003**, *125*, 6368–6369.
11. Kang, Y.-J.; Taton, T. A. Core/Shell Gold Nanoparticles by Self-Assembly and Crosslinking of Micellar, Block-Copolymer Shells. *Angew. Chem., Int. Ed.* **2005**, *44*, 409–412.

12. Hayakawa, T. Fabrication of Self-Organized Chemically and Topologically Heterogeneous Patterns on the Surface of Polystyrene-*b*-Oligothiophene Block Copolymer Films. *Langmuir* **2005**, *21*, 10288–10291.
13. Hayagawa, T.; Horiuchi, S. From Angstroms to Micrometers: Self-Organized Hierarchical Structure within a Polymer Film. *Angew. Chem., Int. Ed.* **2003**, *42*, 2285–2289.
14. Mirjam, W.; Rothe, R.; Landfester, K.; Antonietti, M. Synthesis of Inorganic and Metallic Nanoparticles by Miniemulsification of Molten Salts and Metals. *Chem. Mater.* **2001**, *13*, 4681–4685.
15. Koh, H.-D.; Kang, N.-G.; Lee, J.-S. Fabrication of an Open Au/Nanoporous Film by Water-in-Oil Emulsion-Induced Block Copolymer Micelles. *Langmuir* **2007**, *23*, 12817–12820.
16. Kim, S. W.; Kim, M.; Lee, W. Y.; Hyeon, T. Fabrication of Hollow Palladium Spheres and Their Successful Application to the Recyclable Heterogeneous Catalyst for Suzuki Coupling Reactions. *J. Am. Chem. Soc.* **2002**, *124*, 7642–7643.
17. Khanal, A.; Inoue, Y.; Yada, M.; Nakashima, K. Synthesis of Silica Hollow Nanoparticles Templated by Polymeric Micelle with Core−Shell−Corona Structure. *J. Am. Chem. Soc.* **2007**, *129*, 1534–1535.
18. Willet, N.; Gohy, J.-F.; Auvray, L.; Varshney, S.; Jérôme, R.; Leyh, B. Core−Shell−Corona Micelles by PS-*b*-P2VP-*b*-PEO Copolymers: Focus on the Water-Induced Micellization Process. *Langmuir* **2008**, *24*, 3009–3015.
19. Lei, L.; Gohy, J.-F.; Willet, N.; Zhang, J.-X.; Varshney, S.; Jérôme, R. Tuning of the Morphology of Core−Shell−Corona Micelles in Water. I. Transition from Sphere to Cylinder. *Macromolecules* **2004**, *37*, 1089–1094.
20. Rahman, M. S.; Samal, S.; Lee, J.-S. Synthesis and Self-Assembly Studies of Amphiphilic Poly(*n*-hexyl isocyanate)-*block*-poly(2-vinylpyridine)-*block*-poly(*n*-hexyl isocyanate) Rod−Coil−Rod Triblock Copolymer. *Macromolecules* **2006**, *39*, 5009–5014.
21. Bang, J.; Kim, S. H.; Drockenmuller, E.; Misner, M. J.; Russell, T. P.; Hawker, C. J. Defect-Free Nanoporous Thin Films from ABC Triblock Copolymers. *J. Am. Chem. Soc.* **2006**, *128*, 7622–7629.
22. Gohy, J.-F.; Willet, N.; Lei, Varshney, S.; Jérôme, R. Core−Shell−Corona Micelles with a Responsive Shell. *Angew. Chem., Int. Ed.* **2001**, *40*, 3214–3216.
23. Aizawa, M.; Buriak, J. M. Nanoscale Patterning of Two Metals on Silicon Surfaces Using an ABC Triblock Copolymer Template. *J. Am. Chem. Soc.* **2006**, *128*, 5877–5886.
24. Jeon, S.-H.; Jang, K.-Y.; Lee, S.-H.; Park, H.-W.; Sohn, B.-H. Synthesis of Atypical Nanoparticles by the Nanostructure in Thin Films of Triblock Copolymers. *Langmuir* **2008**, *24*, 11137–11140.
25. Park, S.; Wang, J.-Y.; Kim, B.; Russell, T. P. From Nanorings to Nanodots by Patterning with Block Copolymers. *Nano Lett.* **2008**, *8*, 1667–1672.
26. Wu, M.-L.; Chen, D.-H.; Huang, T.-C. Preparation of Au/Pt Bimetallic Nanoparticles Water-in-Oil Microemulsions. *Chem. Mater.* **2001**, *13*, 599–606.
27. Huang, H.; Hoogenboom, R.; Leenen, M. A. M.; Guillet, P.; Jonas, A. M.; Schubert, U. S.; Gohy, J.-F. Solvent-Induced Morphological Transition in Core-Cross-Linked Block Copolymer Micelles. *J. Am. Chem. Soc.* **2006**, *128*, 3784–3788.